

Performance Evaluation CSMA/CA in MAC Layer and Markov Gaussian Memory Impulse Noise Channels in PHY Layer

Shu-Ming Tseng*, Yung-Chung Wang, Cheng-Yu Yu, and Yu-Fu Liu

Department of Electronic Engineering, National Taipei University of Technology, Taipei 106, Taiwan

*Correspondence: shuming@ntut.edu.tw (S.M.T.)

Abstract—There is memory impulse noise in urban outdoor/indoor mobile channels, underwater acoustic channels, powerline communications (PLC) channels, etc. The prior works about network performance evaluation in impulse noise channels considered both the impulse noise in the physical (PHY) layer and CSMA/CA in the media access control (MAC) layer but they used simpler memoryless impulse noise model. In this paper, we propose to use 3-D Markov chain and power iteration method to analyze the throughput of CSMA/CA protocols with finite queue and more general memory impulse noise. The numerical results show that when the impulse noise is strong (impulse noise to Gaussian noise ratio $R=150$), the normalized throughput would be significantly lower than the case without impulse noise ($R=0$). Therefore, throughput analysis considering the impulse noise effect is essential.

Keywords—memory impulse noise, queuing analysis, carrier-sense multiple access

I. INTRODUCTION

The carrier-sense multiple access/collision avoidance (CSMA/CA) in medium access control (MAC) layer is widely used in Wi-Fi [1–3], IEEE 802.15.4 low-rate wireless personal area networks (WPAN) [4], Internet of Things (IoT) [5], powerline communications (PLC) [6]. Bianchi *et al.* [1] first proposed analysis of the Wi-Fi CSMA/CA protocol using Markov chain (MC) with infinite load and buffer length. One MC represented one station. It evaluated the heavy traffic performance. Liu *et al.* [2] analyzed the performance with finite queue and finite load where each station has the same finite load. It proposed a scheme to reduce the 3-D MC to 2-D one. Sutton *et al.* [3] extended to different finite loads and Rayleigh fading channels. Sutton *et al.* [5] considered IoT devices employing CSMA/CA protocol and their coexistence with other normal Wi-Fi users.

There is impulse noise in many communication systems [7–9] such as urban wireless channels [10, 11], wireless IoT channels [12, 13], PLC channels [14, 15], etc. The impulse noise exists in wireless IoT systems [12, 13] and wired IoT such as PLC systems [16–18]. Bernoulli-

Gaussian (BG) model [6, 19–23] and Middleton Class A model [24–28] are common impulse noise models. However, they are memoryless and cannot represent memory impulse noise for several consecutive samples. Therefore, using Markov-Middleton model [29–31] and Markov-Gaussian model (MG) [32–36] can represent memory impulse noise.

The CSMA/CA in the MAC layer and the impulse noise in the physical (PHY) layer was discussed separately in the networks with the impulse noise. CSMA/CA is commonly used in PLC networks [37–43]. Sheng *et al.* [37] combined time and frequency domain multiplexing for transmission in multi-channel. Mudrievskyi *et al.* [38] proposed CSMA-based backoff algorithm considering priority window used for narrowband (NB) PLC. Ben-Yehzekel *et al.* [39] surveyed MAC protocols including adaptive backoff (ADP), binary exponential backoff (BEB) and additive decrease-multiplicative increase (ADMI) to meet utilities requirement in smart-grid applications. Antonioli *et al.* [40] proposed real-time MAC protocol to enhance security and reliability of HomePlug GP, to reduce energy-consumption. Yoon *et al.* [41] proposed CSMA/CA protocol for OFDM-based PLC system improves the system throughput. Sheng *et al.* [42] and Alvarez *et al.* [43] considered the hybrid PLC/wireless communications for IoT applications but considered the MAC layer only and did not consider the impulse noise the PHY layer.

The previous papers considered either the PHY or MAC layer of the CSMA/CA protocol for the network in the impulse noise channel except [6, 42]. Reddy *et al.* [6] (infinite queue) and Sheng *et al.* [42] (finite queue) considered both the impulse noise in the PHY layer and CSMA/CA in the MAC layer but they used memoryless impulse noise model. In this paper, we proposed the queuing analysis of the CSMA/CA network with finite queue effect in the Markov Gaussian impulse noise channel.

We make the following contribution:

- We propose the power iteration algorithm in Algorithm 1 to directly solve the state probabilities of the 3-D MC and perform queuing analysis of CSMA/CA protocols with finite queue and memory impulse noise by the nature of the sparse matrix. For comparison, Liu *et al.* [2] and Sutton *et al.* [3] collapsed 3-D MC (queue length, backoff stage,

backoff counter) into 2-D one and did not consider the impulse noise. Reddy *et al.* [6] and Sheng *et al.* [42] analyzed performance with memoryless impulse noise. Our previous work [36] was not CSMA/CA mechanism.

- The proposed scheme is simpler than [2] and considers the impulse noise which [2] did not consider. Specifically, in the queueing analysis in Table I, for faster convergence, we propose initializing the elements of v uniformly and for every offered load λ we use the last value of v and p for the previous offered load λ because adjacent offered loads should have close v and p . In addition, the proposed scheme does not need additional matrices B, C, D, and E computation/eigenvector finding/normalizing constant c finding and associated complexity. For example, normalizing constant c finding in Sec. IV B of [2] involved 3-D sum over queue length, backoff stage, and backoff counter.

The rest of this paper is organized as follows. Section II is the system model. Section III is the proposed power iteration algorithm for queueing analysis by 3-D Markov model. Section IV is the numerical result. Section V is the conclusion.

II. SYSTEM MODEL

We first describe the impulse noise model in subsection A, then the packet correct probability in subsection B, and finally the 3D queueing model in subsection C.

A. Markov Gaussian Channel (Memory Impulse Noise) Model

The Markov-Gaussian noise model of two states is shown as Fig. 1. Markov Gaussian channel is a hybrid two state Markov chain and generated by a Gaussian process. The channel state $state1$ represents the Gaussian noise only, and the channel state $state2$ represents the impulse noise. Markov Gaussian channel model describes the burst nature of the channel. First, we assume that the received signal:

$$y = x + n \quad (1)$$

where x is the transmitted signal with bit energy E_b , n is the noise. Then, the probability density functions (PDF) of n are as followings:

$$P(n | state1) = \frac{1}{\sqrt{2\pi\sigma_G^2}} \exp\left\{-\frac{|n|^2}{2\sigma_G^2}\right\} \quad (2)$$

$$P(n | state2) = \frac{1}{\sqrt{2\pi R\sigma_G^2}} \exp\left\{-\frac{|n|^2}{2R\sigma_G^2}\right\} \quad (3)$$

where σ_G^2 is the Gaussian noise variance, and R is the power ratio between the impulse noise and the Gaussian noise. The SNR is defined as $\frac{E_b}{\sigma_G^2}$.

The channel state transition probabilities can be expressed as:

$$P_{j^*|j} = P(state^*|state) \quad state, state^* \in \{1,2\} \quad (4)$$

where $state^*$ is the next state.

\mathbf{M} is the matrix of state transition probabilities of the MG channel:

$$\mathbf{M} = \begin{bmatrix} P_{state1|state1} & P_{state1|state2} \\ P_{state2|state1} & P_{state2|state2} \end{bmatrix} \quad (5)$$

And \mathbf{M} must satisfy:

$$\begin{cases} P_{state1|state1} + P_{state2|state1} = 1 \\ P_{state1|state2} + P_{state2|state2} = 1 \end{cases} \quad (6)$$

In this paper, we let \mathbf{M} be the same as [20, 32, 36]

$$\mathbf{M} = \begin{bmatrix} 0.99 & 0.09 \\ 0.01 & 0.91 \end{bmatrix} \quad (7)$$

Then, channel state probability $\mathbf{P} = [P_{state1} \ P_{state2}]^T$ can be found by

$$\begin{cases} \mathbf{P} = \mathbf{M}\mathbf{P} \\ P_{state1} + P_{state2} = 1 \end{cases} \quad (8)$$

And it can be expressed as:

$$P_{state1} = \frac{P_{state1|state2}}{P_{state2|state1} + P_{state1|state2}} \quad (9)$$

$$P_{state2} = \frac{P_{state2|state1}}{P_{state2|state1} + P_{state1|state2}} \quad (10)$$

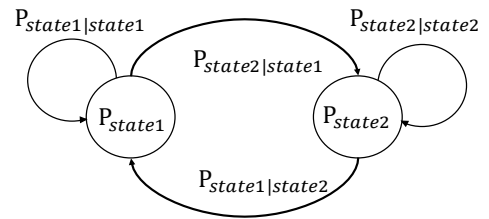


Figure 1. The diagram of two-state Markov chain channel

ω is the channel memory parameter and defined as

$$\omega = \frac{1}{P_{state2|state1} + P_{state1|state2}} \quad (11)$$

Based on the Markov Gaussian channel model, we could compute packet error probability in the following subsection B.

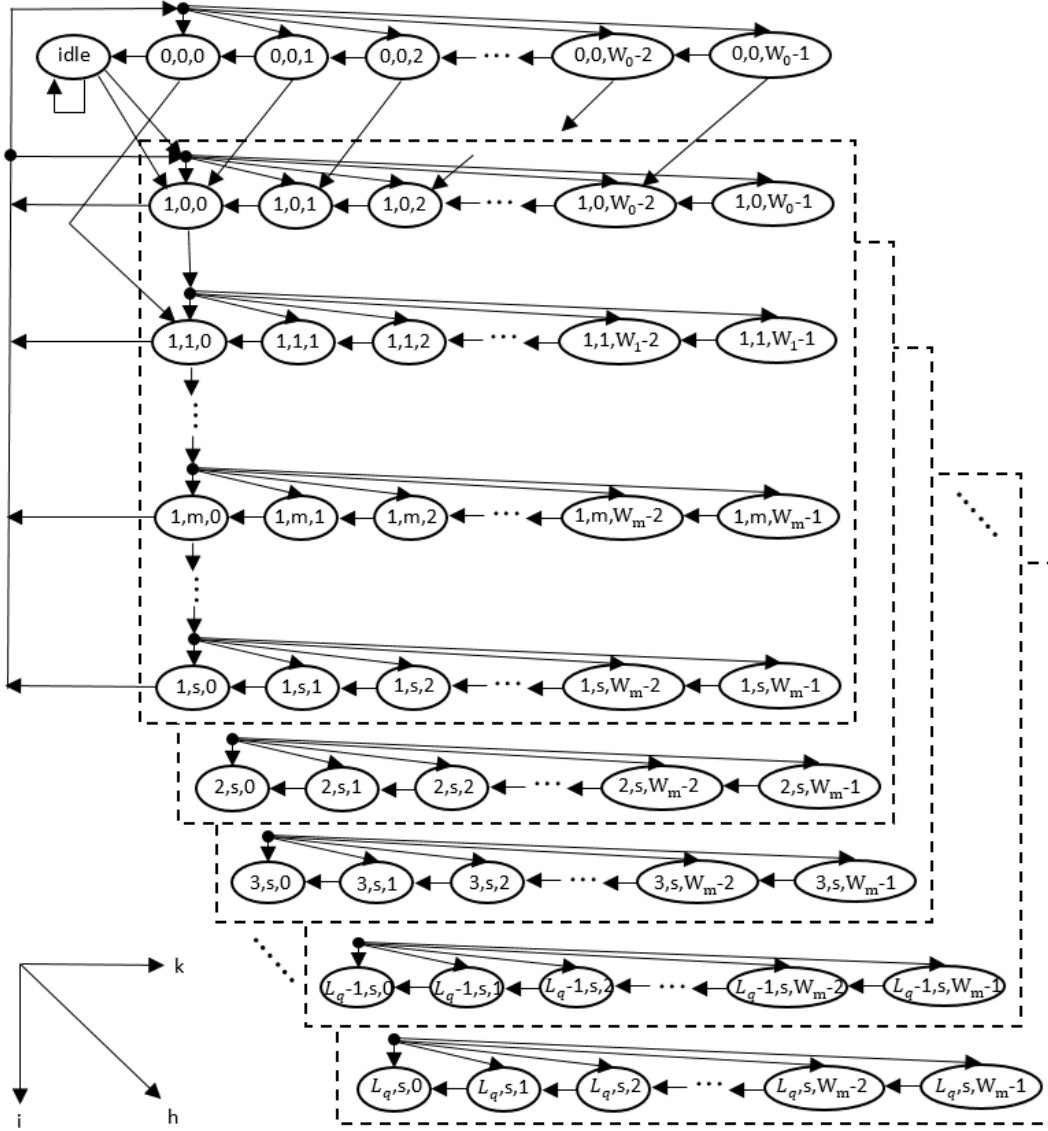


Figure 2. The 3-D Markov chain queueing model.

B. Packet Correct Probability

The bit error probability P_{error_bit} modified from [36, 44]:

$$P_{error_bit}(state1) = Q(\sqrt{SNR}) \quad (12)$$

$$P_{error_bit}(state2) = Q\left(\sqrt{\frac{SNR}{R}}\right) \quad (13)$$

where

$$Q(x) = \frac{1}{\sqrt{2\pi}} \int_x^\infty \exp\left(-\frac{u^2}{2}\right) du \quad (14)$$

We can find the mean of bit error probability $\overline{P_{error_bit}}$ and the mean of packet correct probability $\overline{P_{correct_packet}}$ as follows:

$$\overline{P_{error_bit}} = P_{error_bit}(state1)P_{state1} +$$

$$P_{error_bit}(state2)P_{state2} \quad (15)$$

$$\overline{P_{correct_packet}} = \sum_{l=0}^c \binom{L_{packet}}{l} (\overline{P_{error_bit}})^l (1 - \overline{P_{error_bit}})^{L_{packet}-l} \quad (16)$$

where L_{packet} is packet length, and c is the number of bits the channel code can correct. If the packet has no more c bits in error, the packet transmission is successful.

C. 3-D CSMA/CA Markov Chain Queueing Model

In this subsection, we briefly describe 3-D CSMA/CA MC queueing model in [2]. For details, the readers are referred to [2]. The only differences from the model in [2] is:

- (18) and (19) are corrected, (20) and (21) are unchanged, the boundaries of (22)(23) are

corrected.

- The physical layer parameters, such as the mean of packet correct probability $\overline{P_{correct_packet}}$ in subsection B, are different because the physical layer now have impulse noise

The 2-D CSMA/CA MC model [1] has 2-tuple (i, k) in each 802.11 station. But we consider each station with a finite buffer under finite load, so we should use to 3-D CSMA/CA Markov chain queueing model with 3-tuple (h, i, k) [2]. where h , represents the queue occupying ratio, $0 \leq h \leq L_q$, where L_q is the largest length of queue length, i is used to model the backoff stage, m is maximum contention window exponent, s is maximum times that a packet can retransmit, and they follow $0 \leq i \leq m \leq s$. k is used to model the backoff counter $0 \leq k < W_i$, and W_i is:

$$W_i = 2^{\min(i,m)} W_0 \quad (17)$$

where W_0 is the initial contention windows size.

The 3-D MC is shown in Fig. 2. q_T is the probability which the packet arrives during each transmission state. q is the probability which a packet arrives during each backoff state. p is the probability of a single transmission failure.

The station has a packet arrival, if the channel is not free during the distributed interframe space (DIFS) interval, a backoff is initialized with uniform probability distribution as follow:

$$P[(1,0,k)|(idle)] = \frac{pq}{W_0}, \quad 1 \leq k < W_0, \quad (18)$$

Otherwise

$$P[(1,0,0)|(idle)] = (1-p)q + \frac{pq}{W_0} \quad (19)$$

At backoff stage when queue occupancy does not change or increase.

$$P[(h, i, k-1)|(h, i, k)] = 1 - q \quad (20)$$

$$P[(h+1, i, k-1)|(h, i, k)] = q \quad (21)$$

If the station transmits successfully when backoff counter equals to zero and a new packet arrival or does not.

$$P[(h-1,0,k)|(h,i,0)] = \frac{(1-p)(1-q_T)}{W_0} \quad (22)$$

$$P[(h,0,k)|(h,i,0)] = \frac{(1-p)q_T}{W_0} \quad (23)$$

In contrast, if the station transmits unsuccessfully when backoff counter equals to zero and a new packet arrival or does not.

$$P[(h, i+1, k)|(h, i, 0)] = \frac{p(1-q_T)}{W_{\min(i+1,m)}} \quad (24)$$

$$P[(h+1, i+1, k)|(h, i, 0)] = \frac{pq_T}{W_{\min(i+1,m)}} \quad (25)$$

At the final backoff stage, the state transits back to backoff stage-0, with a new packet arrival or does not.

$$P[(h-1,0,k)|(h,s,0)] = \frac{1-q_T}{W_0} \quad (26)$$

$$P[(h,0,k)|(h,s,0)] = \frac{q_T}{W_0} \quad (27)$$

If the backoff counter is not 0. At $0 < k < W_i$:

$$P[(L_q, i, k-1)|(L, i, k)] = 1 \quad (28)$$

If queue is full during backoff counter equals zero, the station transmits successfully or unsuccessfully. At $0 \leq i < s$:

$$P[(L_q-1,0,k)|(L_q,i,0)] = \frac{(1-p)(1-q_T)}{W_0}, \quad 0 \leq k < W_0 \quad (29)$$

$$P[(L_q,0,k)|(L_q,i,0)] = \frac{(1-p)q_T}{W_0}, \quad 0 \leq k < W_0 \quad (30)$$

$$P[(L_q, i+1, k)|(L_q, i, 0)] = \frac{p}{W_{\min(i+1,m)}}, \quad 0 \leq k < W_{\min(i+1,m)} \quad (31)$$

If no packet is in queue, the station is waiting new packet arrival.

$$P[(0,0,k-1)|(0,0,k)] = 1 - q \quad (32)$$

$$P[(1,0,k-1)|(0,0,k)] = q \quad (33)$$

If the state is (0,0,0), the station is waiting new packet arrival as follows:

$$P[(0,0,k)|(0,0,0)] = \frac{(1-p)q}{W_0}, \quad (34)$$

$$P[(1,1,k)|(0,0,0)] = \frac{pq}{W_1}, \quad (35)$$

$$0 \leq k < W_1$$

If the state return to the idle state

$$P[(idle)|(0,0,0)] = 1 - q \quad (36)$$

$$P[(idle)|(idle)] = 1 - q \quad (37)$$

$$W_i = 2^{\min(i,m)} W_0 \quad (38)$$

III. THE PROPOSED POWER ITERATIVE ALGORITHM FOR QUEUEING ANALYSIS BY 3-D MARKOV CHAIN

The analysis is different from that in [2]. Liu *et al.* [2] did not consider the impulse noise and collapsed 3-D Markov model into 2-D one which involved additional matrices B, C, D, and E computation/eigenvector finding/normalizing constant c finding and associated complexity. For example, normalizing constant c finding in Section IV B of [2] involved 3-D sum over queue length. The proposed scheme considers the impulse noise and is conceptual simpler than [2] because it does not involve additional computation mentioned above.

We consider the impulse noise, so we derive the new value of q_T (the probability that a packet arrives during each transmission state), q (the probability that a packet arrives during each backoff state), and p (the probability of a single transmission failing). For a symmetric network with N stations, the probability of single transmission failing p depends on τ of the other $N-1$ stations:

$$p = 1 - (1 - \tau)^{N-1} \quad (39)$$

where τ is the probability that the station transmits (whether it is successful or not)

$$\tau = 1 - (1 - p)^{\frac{1}{N-1}} \quad (40)$$

We calculate τ from v computed by the power iteration algorithm in Algorithm 1 through summing the probabilities of all states when the backoff counter equals to 0.

The normalized offered load (packet/packet duration) λ is defined:

$$\lambda = N r_q T_{packet} \quad (41)$$

where r_q is arrival rate of packets and T_{packet} is the time spent transmitting payload data (sec)

q_T , the probability that a packet arrives during each transmission state. is defined as :

$$q_T = \min(r_q E_{s|Tx}, 1) \quad (42)$$

where $E_{s|Tx}$, expected time that station is attempting transmission, is

$$E_{s|Tx} = P_{s|Tx} * T_{success} + (1 - P_{s|Tx}) T_{collision} \quad (43)$$

where $T_{collision}$ is the time taken of a collision, $T_{success}$ is the total transmission time of one successful packet, and $P_{s|Tx}$ is the probability of any station in the network producing a successful transmission

$$P_{s|Tx} = (1 - \tau)^{N-1} \overline{P_{correct_packet}} \quad (44)$$

where $\overline{P_{correct_packet}}$ is the mean of packet correct probability.

q , the probability that a packet arrives during each transmission state., is defined as:

$$q = \min(r_q E_{s,N-1}, 1) \quad (45)$$

To obtain $E_{s,N-1}$, expected time taken per 3-D MC queueing model state for $N - 1$ stations system, we first consider $E_{s,N}$, the expected time spent per 3-D Markov chain queueing model state for N stations system,

$$E_{s,N} = P_{noTx,N} \sigma + P_{success,N} T_{success} + P_{collision,N} T_{collision} \quad (46)$$

$P_{noTx,N}$, probability that no station is transmitting for the N stations system, $P_{success,N}$, probability when any station transmits successfully for the N stations system, and $P_{collision,N}$, probability when there is a collision due to two or more stations transmit simultaneously for N stations system, are defined respectively as:

$$P_{noTx,N} = (1 - \tau)^N \quad (47)$$

$$P_{success,N} = N \tau (1 - \tau)^{N-1} \overline{P_{correct_packet}} \quad (48)$$

$$P_{collision,N} = 1 - P_{noTx,N} - P_{success,N} \quad (49)$$

Then, we similarly obtain $E_{s,N-1}$, $P_{noTx,N-1}$, $P_{success,N-1}$ and $P_{collision,N-1}$ for $N-1$ stations system to be used for q :

$$E_{s,N-1} = P_{noTx,N-1} \sigma + P_{success,N-1} T_{success} + P_{collision,N-1} T_{collision} \quad (50)$$

$$P_{noTx,N-1} = (1 - \tau)^{N-1} \quad (51)$$

$$P_{success,N-1} = (N - 1) \tau (1 - \tau)^{N-2} \overline{P_{correct_packet}} \quad (52)$$

$$P_{collision,N-1} = 1 - P_{noTx,N-1} - P_{success,N-1} \quad (53)$$

And throughput can be calculated:

$$throughput = \frac{T_{packet}}{E_{s,N}} \quad (54)$$

Table I is the proposed power iterative algorithm to solve 3-D MC to analyze the throughput and delay. Originally, power iteration is one of PageRank calculation method [45, 46]. PageRank was used to rank web pages in Google search outcomes.

First, define v as 1-D vector of probabilities of all CSMA/CA states, and A is the state transition probability matrix, In A , the sum of each column must equal to one and $|v|=1$. And it must satisfy

$$v = Av \quad (55)$$

Algorithm 1. The Proposed Power Iteration Algorithm

Initialization:
 Let each element of v be equal to: $\frac{1}{\text{number of elements of } v}$.

Let p be a small value, the normalized offered load λ is a small value.
 Note: uniformly initialization of each element of v for faster convergence^a

Loop:
 1:for each λ :
 2: repeat
 3: calculate q_T, q , and find A .
 4: repeat
 5: $v = Av$
 6: until v converge
 7: use v to calculate τ , and find new p
 8: until p converges
 9: calculate throughput
 10:endifor

Note: at every loop λ , we use the last value (previous λ) of v and p and can significantly reduce the number of iterations and run much faster.
 As shown above, we don't re-initialized value of v and p .

TABLE I. THE ANALYSIS AND SIMULATION PARAMETERS

Parameter	Value
STA (the number of stations)	20
N	10
L_{packet}	8192(bits)
Data rate	11(Mbps)
T_{packet}	$L_{\text{packet}}/\text{Data rate}$
s (maximum retransmission)	7
Slot time	20 μ s
DIFS	50 μ s
SIFS	10 μ s
L_q	50
RTS	160 μ s
CTS	112 μ s
ACK	112 μ s
CW_{min}	32
CW_{max}	1024
SNR	30 dB
T_{success}	DIFS+RTS+3SIFS+CTS+ T_{packet} +ACK
$T_{\text{collision}}$	DIFS+RTS
R	150
ω	10

If $v=Av$, equation is established, and then $(I-A)v=0$, where I is an identity matrix. It is a linear dependence equation, so it has more than one solution. However, $|v|=1$ and the sum of each column of A is equal to one, so it has unique solution.

IV. NUMERICAL RESULTS

The simulation parameters are the same as IEEE 802.11b specification, as shown in Table I. The channel memory parameters $\omega = 10$, the channel state probability $P_{\text{state1}}=0.9, P_{\text{state2}}=0.1$, and the channel state transition probabilities matrix A are same as [20, 32].

$$A = \begin{bmatrix} 0.99 & 0.09 \\ 0.01 & 0.91 \end{bmatrix} \quad (56)$$

For SNR=30dB, the simulation and numerical results of the throughput for different R, R=0, 50, 100, 150 is shown in Figs. 3–6, respectively.

In Fig. 3, when the ratio of impulse noise over Gaussian noise R=0 (without impulse noise), our numerical results are those of the classical scheme in [2] which assume no impulse noise. In other words, Scheme in [2] is a special case (R=0) of our proposed scheme. In Figs. 4–6, where the ratio of impulse noise over Gaussian noise R=50,100,150, respectively, we can see that for larger impulse noise (larger R), the throughput is lower.

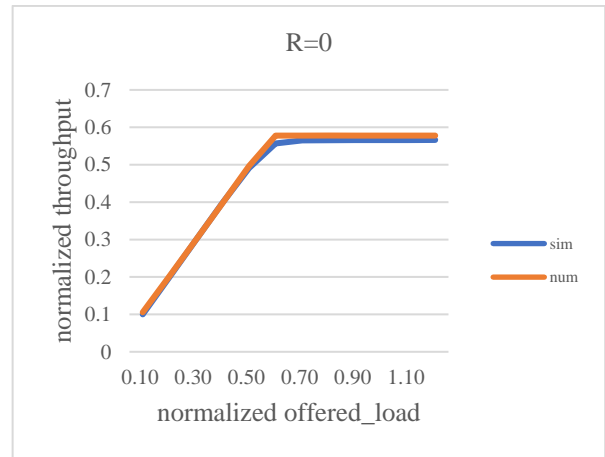


Figure 3. Simulated/numerical throughput without impulse noise (the ratio of impulse noise over Gaussian noise R=0). our simulation results and numerical results are those of the classical scheme in [2] which assume no impulse noise. In other words, Scheme in [2] is a special case (R=0) of our proposed scheme.

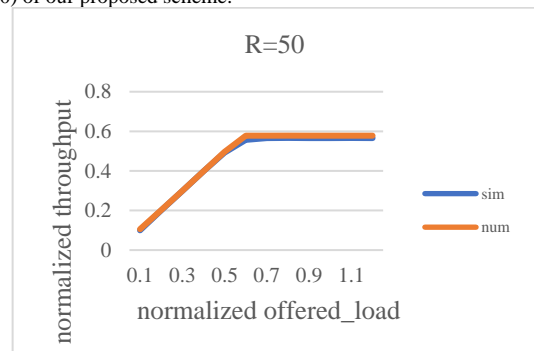


Figure 4. Simulated/numerical throughput for R=50.

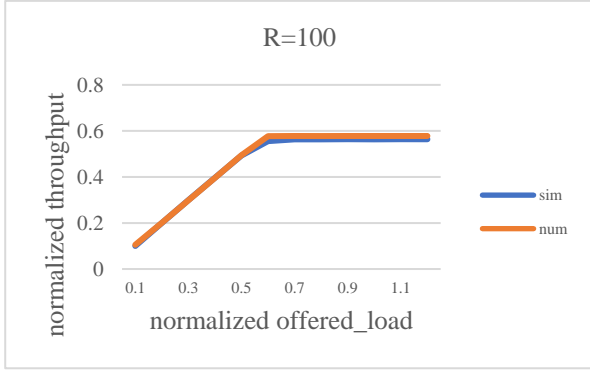


Figure 5. Simulated/numerical throughput for R=100.

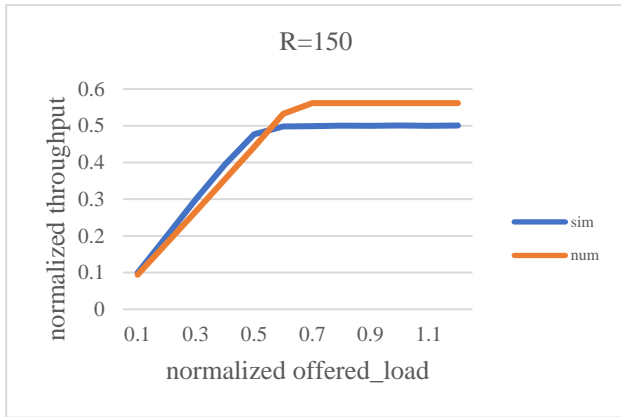


Figure 6. Simulated/numerical throughput with impulse noise R=150.

A. The Complexity Analysis

The matrix A is sparse. The A has $\{1 + W_0 + L_q W_0 [(s - m + 2)2^m - 1]\}^2$ elements, and the number of non-zero elements is $(2L_q - 1)[(s - m + 2)2^{m+1} - s - 1] + (2L_q s - 4L_q + 9)W_0$. According to the analysis and simulation parameters in Table I (similar to IEEE 802.11b and [2]), the A has $4.1304e+10$ elements and has only 826504 non-zero elements, so the compression ratio is $2.0010e-5$, it is very sparse. We can use sparse matrix to significantly reduce the time complexity and space complexity.

B. Related Discussions on Numerical Results

In [6, 42] they considered throughput analysis of CSMA/CA mechanism with memoryless impulse noise in PLC. Tseng *et al.* [36] analyzed and simulated the throughput of DS CDMA/slotted ALOHA networks with Markov Gaussian memory impulse noise but not the CSMA/CA protocol. Unlike previous research [6, 36, 42], in this paper, we propose 3-D CSMA/CA Markov chain queueing model to analyze CSMA/CA mechanism with Markov Gaussian memory impulse noise and finite queue effect for PLC networks. We propose to use the sparse matrix and power iteration algorithm to reduce the time complexity and the space complexity of the throughput analysis.

The numerical results show that when the impulse to Gaussian noise ratio R increases, the throughput decreases especially when strong impulse noise $R=150$ (simulated normalized throughput=0.5). In Fig. 6, the gap between

analytical and simulated throughput is larger because we approximate the bit error probability under the impulse noise by the mean of it as shown in Eq. (15)–Eq. (16). We would have a 4-D Markov chain if we take the state of the impulse noise into consideration. The price of approximation is the accuracy loss at $R=150$. One future direction is to extension to 4-D Markov chain model to get accurate analyzed throughput, Besides, another future research direction is to consider CSMA/CA and more advanced PHY layer technology such as multiple-input multiple-output (MIMO) for higher throughput in beyond 5G communication systems [47–53].

V. CONCLUSION

In this paper, we propose 3-D CSMA/CA Markov chain queueing model to analyze CSMA/CA mechanism with Markov Gaussian impulse noise and finite queue effect for PLC networks. We propose to use the sparse matrix and power iteration algorithm to reduce the time complexity and the space complexity of the throughput analysis. The results show that when there is strong memory impulse noise ($R=150$), the simulated normalized throughput would be significantly lower than the case without impulse noise ($R=0$). Therefore, throughput analysis considering the impulse noise effect is essential. The research limitation of this paper is that we restrict to 3-D Markov chain for throughput analysis in this paper, so the deviation of simulated and analyzed normalized throughput is notably larger when the intensity of impulse noise is large.

CONFLICT OF INTEREST

The authors declare no conflict of interest

AUTHOR CONTRIBUTIONS

Conceptualization, methodology, and formal analysis, Shu-Ming Tseng and Yung-Chung Wang; software and data curation, Cheng-Yu Yu and Yu-Fu Liu; All authors have read and agreed to the published version of the manuscript.

FUNDING

This research was funded by National Science and Technology Council, NSTC 112-2221-E-027-079-MY2, and NTUT-BJUT Joint Program, NTUT-BJUT-112-02.

REFERENCES

- [1] G. Bianchi, "Performance analysis of the IEEE 802.11 distributed coordination function," *EEE Journal on Selected Area in Commun.*, vol. 18, no. 3, 2000.
- [2] R. P. Liu, G. J. Sutton, and I. B. Collings, "A new queueing model for QoS analysis of IEEE 802.11 DCF with finite buffer and load," *IEEE Trans. Wireless Comm.*, vol. 9, no. 8, pp. 2664–2675, Aug. 2010.
- [3] G. J. Sutton, R. P. Liu, and I. B. Collings, "Modelling IEEE 802.11 DCF heterogeneous networks with Rayleigh fading and capture," *IEEE Trans. Commun.*, vol. 61, no. 8, pp. 3336–3348, Aug. 2013.
- [4] T. R. Park *et al.*, "Throughput and energy consumption analysis of IEEE 802.15.4 slotted CSMA/CA," *Electronics Letters*, vol. 41, no. 18, pp. 1017–1019, Sep. 2005.

- [5] G. J. Sutton, R. P. Liu, and Y. J. Guo, "Harmonising coexistence of machine type communications with Wi-Fi data traffic under frame-based LBT," *IEEE Transactions on Communications*, vol. 65, no. 9, pp. 4000–4011, Sept. 2017.
- [6] Y. S. Reddy, A. Dubey, and A. Kumar, "A MAC-PHY cross-layer analysis of NB-PLC system in presence of impulsive noise," in *Proc. 10th Int. Conf. Commun. Syst. Netw.*, Bengaluru, India, pp. 384–387, 2018.
- [7] X. Wang and R. Chen, "Blind turbo equalization in Gaussian and impulsive noise," *IEEE Transactions on Vehicular Technology*, vol. 50, no. 4, pp. 1092–1105, July 2001.
- [8] E. Axell, K. C. Wiklundh and P. F. Stenumgaard, "Optimal power allocation for parallel two-state Gaussian mixture impulse noise channels," *IEEE Wireless Communications Letters*, vol. 4, no. 2, pp. 177–180, April 2015.
- [9] E. Axell, P. Eliardsson, S. Ö. Tengstrand, and K. Wiklundh, "Power control in interference channels with class A impulse noise," *IEEE Wireless Communications Letters*, vol. 6, no. 1, pp. 102–105, Feb. 2017.
- [10] K. L. Blackard, T. S. Rappaport, and C. W. Bostian, "Measurements and models of radio frequency impulsive noise for indoor wireless communications," *IEEE J. Select. Areas Commun.*, vol. 11, pp. 991–1001, Sept. 1993.
- [11] T. K. Blankenship, D. M. Krizman, and T. S. Rappaport, "Measurements and simulation of radio frequency impulsive noise in hospitals and clinics," in *Proc. 1997 IEEE Vehicular Technology Conf. (VTC'97)*, Phoenix, AZ, May 1997, pp. 1942–1946.
- [12] I. Landa, A. Blázquez, M. Vélez, and A. Arrinda, "Indoor measurements of IoT wireless systems interfered by impulsive noise from fluorescent lamps," in *Proc. 2017 11th European Conference on Antennas and Propagation (EUCAP)*, Paris, 2017, pp. 2080–2083.
- [13] H. Li *et al.*, "Measurement and characterization of electromagnetic noise in edge computing networks for the industrial internet of things," *Sensors*, vol. 19, no. 14, p. 3104, 2019.
- [14] D. F. Tseng, F. G. Mengistu, Y. S. Han, M. A. Mulatu, L. C. Chang, and T. R. Tsai, "Robust turbo decoding in a Markov Gaussian channel," *IEEE Wireless Communications Letters*, vol. 3, no. 6, pp. 633–636, 2014.
- [15] S. M. Tseng, D. F. Tseng, T. R. Tsai, and Y. H. S. Han, "Robust turbo decoding in single-carrier systems over memoryless impulse noise channels," in *Proc. 2016 International Conference on Advanced Technologies for Communications (ATC 2016)*, Hanoi, Vietnam, Oct. 12–14, 2016, pp. 344–349.
- [16] V. Fernandes, H. V. Poor, and M. V. Ribeiro, "A hybrid power line/wireless dual-hop system with energy harvesting relay," *IEEE Internet of Things Journal*, vol. 5, no. 5, pp. 4201–4211, Oct. 2018.
- [17] A. Ikpehai, B. Adebisi, and K. Anoh, "Can 6LoPLC enable indoor IoT?," in *Proc. 2019 IEEE International Symposium on Power Line Communications and its Applications (ISPLC)*, Praha, Czech Republic, 2019, pp. 1–6.
- [18] A. Ghiasimonfared, D. Righini, F. Marcuzzi, and A. M. Tonello, "Development of a hybrid LoRa/G3-PLC IoT sensing network: An application oriented approach," in *Proc. 2017 IEEE International Conference on Smart Grid Communications (SmartGridComm)*, Dresden, Germany, 2017, pp. 503–508.
- [19] S. P. Herath, N. H. Tran, and T. Le-Ngoc, "On optimal input distribution and capacity limit of Bernoulli-Gaussian impulsive noise channels," in *Proc. the 2012 IEEE International Conference on Communications*, Ottawa, ON, Canada, June 10–15, 2012, pp. 3429–3433.
- [20] M. Ghosh, "Analysis of the effect of impulse noise on multicarrier and single carrier QAM systems," *IEEE Trans. Commun.*, vol. 44, no. 2, pp. 145–147, Feb. 1996.
- [21] T. Shongwe, A. J. H. Vinck, and H. C. Ferreira, "On impulse noise and its models," in *Proc. the 2014 IEEE International Symposium on Power Line Communications*, 2014, pp. 12–17.
- [22] Bin Han, Yang Lu, Kai Wan, Hans D. Schotten. "A fast blind impulse detector for Bernoulli-Gaussian noise in underspread channel." in *Proc. 2018 IEEE International Conference on Communications (ICC)*, IEEE, 2018.
- [23] R. Bale, T. S. Seetharamaiah, Y. S. Reddy, A. Dubey, and T. Panigrahi, "OFDM vs FBMC: A comparative analysis for broadband-PLC," in *Proc. 2018 10th International Conference on Communication Systems and Networks (COMSNETS)*, Bengaluru, 2018, pp. 480–483.
- [24] D. Middleton, "Statistical-physical models of electro-magnetic interference," *IEEE Trans. Electromagn. Compat.*, vol. EMC-19, no. 3, pp.106–126, Aug. 1977.
- [25] P. Lu, Z. Luo, and Y. Zhang, "The Gaussianization and generalized matching method for robust detection in impulsive noise," in *Proc. 14th IEEE ICSP*, Beijing, China, Aug. 2018, pp. 727–732.
- [26] Al-Rubaye, Ghanim A, Charalampos C. Tsimenidis, and Martin Johnston. "Performance evaluation of T-COFDM under combined noise in PLC with log-normal channel gain using exact derived noise distributions," *IET Communications*, pp.766–775, 2019.
- [27] F. Rouissi *et al.*, "Statistical analysis of the Middleton Class-A noise effects on multi-carrier OFDM-based communication system," *Telecommunication Systems*, vol. 82, pp. 115–123, 2023.
- [28] M. Hasan *et al.*, "Performance evaluation of OFDM vs FBMC in impulsive noise channel," *Journal of Optoelectronics and Communication*, vol. 5, pp. 18–25, 2023.
- [29] G. Ndo, F. Labeau, and M. Kassouf, "A markov-middleton model for bursty impulsive noise: Modeling and receiver design," *IEEE Transactions on Power Delivery*, vol. 28, no. 4, pp. 2317–2325, Oct. 2013.
- [30] P. Amirshahi, S. M. Navidpour, and M. Kavehrad, "Performance analysis of uncoded and coded OFDM broadband transmission over low voltage power-line channels with impulse noise," *IEEE Trans. Power Del.*, vol. 21, no. 4, pp. 1927–1934, Oct. 2006.
- [31] T. Shongwe, A. J. H. Vinck, and H. C. Ferreira. "A study on impulse noise and its models," *SAIEE Africa Research Journal*, vol. 106, no. 3, pp.119-131, September 2015.
- [32] D. Fertanani and G. Colavolpe, "On reliable communications over channels impaired by bursty impulse noise," *IEEE Trans. Commun.*, vol. 57, no. 7, pp. 2024–2030, Jul. 2009.
- [33] H. Barka, M. S. Alam, G. Kaddoum, F. Sacuto and B. L. Agba, "BNET: A neural network approach for IIR-based detection in the presence of bursty impulsive noise," *IEEE Wireless Communications Letters*, vol. 12, no. 1, pp. 80–84, Jan. 2023,
- [34] S. Tseng *et al.*, "Deep learning based decoding for polar codes in markov GAUSSIAN memory impulse noise channels," *Wireless Personal Communications*, vol. 122, pp. 737–753, 2022.
- [35] S. Nlend *et al.*, "Access convergence for heavy load markov ethernet bursty traffic using two-level statistical multiplexing," *ECTI Transactions on Electrical Engineering, Electronics, and Communications*, vol. 20, pp. 358–370, 2022.
- [36] S. M. Tseng, Y. C. Wang, C. W. Hu, and T. C. Lee, "Performance analysis of CDMA/ALOHA networks in memory impulse channels," *Mathematical Problems in Engineering*, p. 9373468, June 2018.
- [37] Z. Sheng, A. Kenarsari-Anhari, N. Taherinejad, and V. C. M. Leung, "A multichannel medium access control protocol for vehicular power line communication systems," *IEEE Trans. Veh. Technol.*, vol. 65, no. 2, pp. 542–554, Feb. 2016.
- [38] S. Mudrievskiy, I. Tsokalo, A. Haidine, B. Adebisi, and R. Lehnert, "Performance evaluation of MAC backoff algorithm in narrowband PLC," in *Proc. IEEE International Conference on Smart Grid Communications (SmartGridComm)*, pp. 108–113, Brussels, Oct. 2011.
- [39] Y. Ben-Yehzekel, R. Gazit, and A. Haidine, "Performance evaluation of medium access control mechanisms in high-speed narrowband PLC for smart grid applications," in *Proc. IEEE Int. Symp. Power Line Commun. Appl.*, Beijing, China, Mar. 2012, pp. 94–101.
- [40] R. P. Antonioli, M. Roff, Z. Sheng, J. Liu, and V. C. M. Leung, "A real-time MAC protocol for in-vehicle power line communications based on HomePlug GP," in *Proc. IEEE Veh. Technol. Conf.*, May 2015, pp. 1–5.
- [41] S. G. Yoon, D. Kang, and S. Bahk, "OFDMA CSMA/CA protocol for power line communication," in *Proc. Int. Symp. Power Line Commun. Appl.*, Rio de Janeiro, Brazil, Mar. 2010, pp. 297–302.
- [42] H. Sheng *et al.*, "A CSMA/CA based MAC protocol for hybrid power-line/visible-light communication networks: Design and analysis," *Digital Communications and Networks, Early Access*, 2023.
- [43] L. B. Alvarez *et al.*, "CSMA/CA protocol design in hybrid network of Visible Light Communication and RF Femtocell systems," *Optics Communications*, vol. 537, 129434, 2023.

- [44] J. M. Holtzman, "A simple, accurate method to calculate spread spectrum multiple access error probabilities," *IEEE Trans. Commun.*, vol. 40, pp. 461–464, Mar. 1991.
- [45] T. Haveliwala, S. Kamvar, D. Klein, C. Manning, and G. Golub, "Computing PageRank using Power Extrapolation," Technical Report, Stanford University, 2003.
- [46] PageRank. [Online]. Available: <https://zh.wikipedia.org/wiki/PageRank>
- [47] Y. H. Chen *et al.*, "Low complexity user selection and power allocation for uplink NOMA beamforming systems," *Wireless Personal Communications*, vol. 111, pp. 1413–1429, April 2020.
- [48] B. -Y. Chen *et al.*, "Hybrid beamforming and data stream allocation algorithms for power minimization in multi-user massive MIMO-OFDM systems," *IEEE Access*, vol. 10, pp. 101898–101912, Sep. 2022.
- [49] N. H. Cheng *et al.*, "Maximum likelihood-based adaptive iteration algorithm design for joint CFO and channel estimation in MIMO-OFDM systems," *EURASIP J. Adv. Signal Process.*, vol. 2021, 6, Jan. 2021.
- [50] S. M. Tseng *et al.*, "Cross-layer resource management for downlink BF-NOMA-OFDMA video transmission systems and supervised/unsupervised learning based approach," *IEEE Transactions on Vehicular Technology*, vol. 71, no. 10, pp. 10744–10753, Oct. 2022.
- [51] E. Trinidad and L. Materum, "High-accuracy visualization-based grouping of MIMO multipath waves," *Journal of Communications*, vol. 18, pp. 68–75, 2023.
- [52] A. Teologo and L. Materum, "Accuracy and cluster analysis of 5.3 GHz indoor and 285 MHz semi-urban MIMO LOS and NLOS propagation multipaths," *Journal of Communications*, vol. 18, pp. 135–139, 2023.
- [53] G. Hussain *et al.*, "Filtered OFDM system improvement using hamming code," *Journal of Communications*, vol. 18, pp. 215–220, 2023.

Copyright © 2023 by the authors. This is an open access article distributed under the Creative Commons Attribution License ([CC BY-NC-ND 4.0](https://creativecommons.org/licenses/by-nc-nd/4.0/)), which permits use, distribution and reproduction in any medium, provided that the article is properly cited, the use is non-commercial and no modifications or adaptations are made.